

POROUS SILICON (P-TYPE) PREPARED BY ELECTROCHEMICAL ETCHING AND STUDY OF STRUCTURE AND MORPHOLOGY PROPERTIES AND EFFECT OF NEUTRON IRRADIATION

A. A. SULAIMANA^a, M. M. ALYAS^{a,*}, A. M. MUHAMMED^b

^a*Department of Physics, College of Science, Mosul University, Iraq*

^b*Sumy State university Technical , Sumy, Ukraine*

The research of electrochemical cell (ECE) for etching time (10 , 20 and 30 min.) of the porous silicon (p-type) was fabricated by. This techniques and study at room temperature the irradiated by using neutron with flux density up $10^{12} \text{ cm}^{-2} \text{ s}^{-1}$ of high energy. The crystallographic structure and morphological properties of P-Si were investigated by X-ray diffraction (XRD) and Scanning electron microscope techniques before and after irradiation. The experimental results of X-ray reveal that P-Si layer still in crystallize phase and nano range. The morphological properties (Top surface and cross section) of P-Si layer were investigated by field emission Scanning electron microscope (FESEM) technique, these images illustrate that the pores diameter increase with height etching time. Finally , these results enhanced of the P-Si substrate after the irradiation. The effect of irradiation were best of structure of P-Si.

(Received March 21, 2019; Accepted January 7, 2020)

Keywords: porous silicon, electrochemical etching, neutron irradiation.

1. Introduction

Crystalline silicon (C-Si) is an important material of the last century that has been the corner stone of the semiconductor industry and has spear headed extraordinary technological advancement [1]. Silicon nanostructures have attracted a great attention as well as tremendous efforts since those promising materials could be used in many important applications[2]. Porous silicon were addressed due to their potential applications for example , piezoelectric transducers [3], light visual guide [4], surface ultrasound mechanics [5], gas sensors conductive [6]. P-Si is a complex network of pores separated by thin walls consisting of these nanostructures. The reduction in the size of the semiconductors to the nano-scale sizes is accompanied by significant modifications in their electronic, optical and electrical properties. Therefore, quantum confinement effects in such systems offer many possibilities for tailoring the optical and electrical properties for specific applications [7].The research on investigating effect irradiation in semiconductor for different types of irradiation including electrons, ions and neutrons on properties of semiconductor . [8-9]. Research on semiconductor receptors based on the effect of radiation which focuses on the operation of the electrical devices and the electrical conductivity of the materials have been evaluated with the assessment of the effect of radiation .Most defects are caused by exposure to high energy radiation (i.e., displacement damage) and the generation of photoelectrons [10-11]. The properties of materials used in photonic devices are modified by introducing absorption range or color centers that are a source of concern for these deviees . [12].

In this study we were illustrated PSi by electrochemical anodization method and exploring influence of neutron irradiation on the surface of PSi and characterizing any surface changes due to irradiation as (crystalline size, pore diameter) using analytical techniques, such as XRD, FESEM (Top surface)and (cross section). These techniques were used to investigate the structural and morphological properties of porous silicon samples without and with influence of irradiation.

* Corresponding author: mohanad.moaid@yahoo.com

2. Experimental

Prepared of P-Si with resistivity (0.02- 0.04 Ω cm) by anodization electrochemical etching of p-type Si (111), etching time (10, 20 and 30 min.), current density (30 mA/cm²) and fixed electrolyte solution HF : C₂H₅OH (1:4). Ethanol is added to the aqueous solution. They immediately removed if ethanol is present. This is reason, To promote bubble removal it anodization cell is design in careful of the important. The HF acid with not interaction the Teflon therefore the cell made it, before in the upper part of cell used rubber O-ring. central circular of (1.5 cm²) of The Teflon has a to allow touching the wafer Si. To apply current across the cell used to the two electrodes. Gold mesh of the first (upper) is connected with the solution HF and the second of stainless still (lower) is foil below wafer Si. In the end process etching, the sample were rinsed with ethanol and pentane and dried by nitrogen. To know and clarify of irradiation on P-Si layer after the effect of irradiation on P-Si surface at room temperature. The structure of the P-Si was determined by X-ray diffraction measurements with XRD.

3. Results and discussion

3.1. Structure properties

X-ray diffraction is used to determine the nature of different materials and phases in a sample. X-ray diffraction was investigated of P-Si layers without and with irradiation with neutron flux density. Fig. (1) illustrates XRD of the P-Si sample before irradiation, P-Si sample has a maximum diffraction peak at (111) corresponds $2\theta = 28.35^\circ$ and other peaks at (220),(331),(400) and (422) observed at 47.32° , 57.75° , 69.31° and 88.52° respectively as Fig.1 (A), we note that the full width half maximum (FWHM) increases with increasing etching time. Also, diffraction peaks were shifted with etching time. as Fig. 1(b and c), which means that the porous silicon layers crystallized in the phase (crystalline structure). The increasing in etching time lead to increase the number of pores and also produces a pore at large size. The data are in agreement with the (JCPDS) card for P-Si. On the other hand, after irradiation, Fig. (2) notes appearance anew diffraction peak (200) instead of (331) at $2\theta = 34.22^\circ$, this happens due to the change in the phase. The relative intensity of distinctive (200) and other peaks (111), (220), (400) and (422) were increased compared with samples before irradiation, increasing of the process of irradiation effected the formation of P-Si relative intensity of each peak. Also, the effect of irradiation power produces decreasing of energy gap. This is attributed to interface in localization of the initiation of pores leading to reduce the wall between them [13] as Fig.2(A₁,b₁ and c₁).

To find L (the crystallites size) of P-Si measurement the full width half maximum (FWHM) of the peak by Scherer Equation [14]:

$$L = \frac{k\lambda}{B \cos\theta} \quad (1)$$

θ = the angle of scattering, λ = X-ray of the wavelength (0.154 nm), L = is crystallites size (nm) and (B) is FWHM and (k) is a constant ($k = 0.89$). We can be calculated the energy gap of layer P-Si [16]:

$$E_g^* = E_g + \frac{88.34}{L^{(1.37)}} \quad (2)$$

E_g^* (eV) energy band gap of P-Si layer, E_g (eV) energy band gap of bulk.

Table (1) the values of FWHM (nm), L (nm) and E_g^* (eV) before irradiation, the values of

FWHM and energy gap increase with etching time. This occurs due to the broadening of the inter connection between the pore channel, while after irradiation [15].

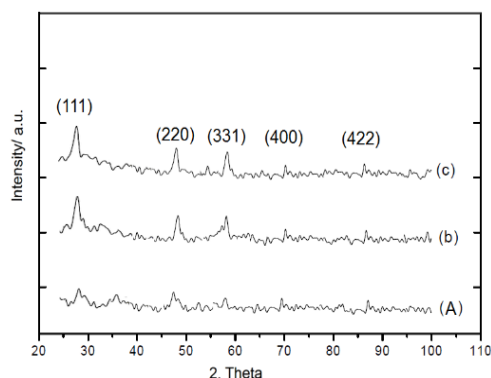


Fig. 1. XRD pattern at etching time 10, 20 and 30 min of porous silicon without irradiation.

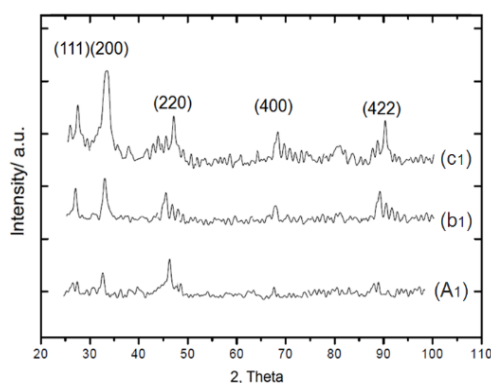


Fig. 2. XRD pattern at etching time 10, 20 and 30 min. of P-Si after neutron irradiation

Table 1. XRD results at etching time 10, 20 and 30 min of P-Si before neutron irradiation.

| Sample (p-PSi) | hkl | 2θ (deg.) | FWHM (deg.) | L (nm) | Eg*(eV) |
|----------------|-------|-----------|-------------|--------|---------|
| A | (111) | 28.35 | 0.60 | 2.79 | 1.721 |
| | (220) | 47.32 | 0.57 | 2.23 | 1.726 |
| | (331) | 57.75 | 0.59 | 2.15 | 1.729 |
| | (400) | 69.31 | 0.61 | 2.14 | 1.731 |
| | (422) | 88.52 | 0.62 | 2.1 | 1.737 |
| B | (111) | 28.31 | 0.63 | 2.77 | 1.862 |
| | (220) | 47.28 | 0.59 | 2.21 | 1.868 |
| | (331) | 54.68 | 0.60 | 2.11 | 1.869 |
| | (400) | 74.25 | 0.62 | 2.09 | 1.875 |
| | (422) | 87.48 | 0.63 | 2.04 | 1.882 |
| C | (111) | 28.12 | 0.65 | 2.71 | 2.112 |
| | (220) | 47.1 | 0.61 | 2.1 | 2.136 |
| | (331) | 54.27 | 0.64 | 1.97 | 2.142 |
| | (400) | 74.1 | 0.66 | 1.94 | 2.181 |
| | (422) | 87.17 | 0.69 | 1.92 | 2.194 |

Table 2. XRD results at etching time 10, 20 and 30 min of P-Si after neutron irradiation.

| Sample (p-PSi) | hkl | 2 θ (deg.) | FWHM (deg.) | L (nm) | E _g *(eV) |
|----------------|-------|-------------------|-------------|--------|----------------------|
| A ₁ | (111) | 28.21 | 0.47 | 4.79 | 1.531 |
| | (200) | 34.22 | 0.52 | 4.81 | 1.537 |
| | (220) | 47.22 | 0.49 | 4.83 | 1.539 |
| | (400) | 68.76 | 0.53 | 4.84 | 1.547 |
| | (422) | 88.42 | 0.54 | 4.85 | 1.554 |
| b ₁ | (111) | 28.16 | 0.45 | 4.86 | 1.713 |
| | (200) | 33.87 | 0.49 | 4.92 | 1.722 |
| | (220) | 46.95 | 0.47 | 4.97 | 1.734 |
| | (400) | 68.27 | 0.48 | 5.12 | 1.753 |
| | (422) | 88.13 | 0.5 | 5.23 | 1.778 |
| c ₁ | (111) | 28.11 | 0.43 | 5.13 | 1.923 |
| | (200) | 33.67 | 0.47 | 5.17 | 1.932 |
| | (220) | 46.27 | 0.46 | 5.31 | 1.952 |
| | (400) | 68.11 | 0.48 | 5.54 | 1.962 |
| | (422) | 87.77 | 0.49 | 5.56 | 1.977 |

3.2. Morphological properties

a) Top surface images of P-Si

FESEM of the P-Si samples before and after irradiation was carried out using field emission at different etching time (10, 20 and 10 min.) with neutron flux density. Fig. (3) shows FESEM of the P-Si without irradiation, the layer of P-Si is non-uniform and has irregular shape. The important etching parameters. The pores in the P-Si are seen as dark dots as Fig.3 (a), diameter of P-Si increases with time as Fig.3 (b). This largeness of width increase in holes number on the surface of P-Si with etching time. After irradiation, Fig. (4) shows pore-like spherical shape elongated and the defect clusters of P-Si samples were large than those of the samples before irradiation as Fig.4 (a₁), also, pore width was increased with increasing etching time, since the radiation reduces the thin walls between neighbor pores as Fig.4 (b₁ and c₁) [17].

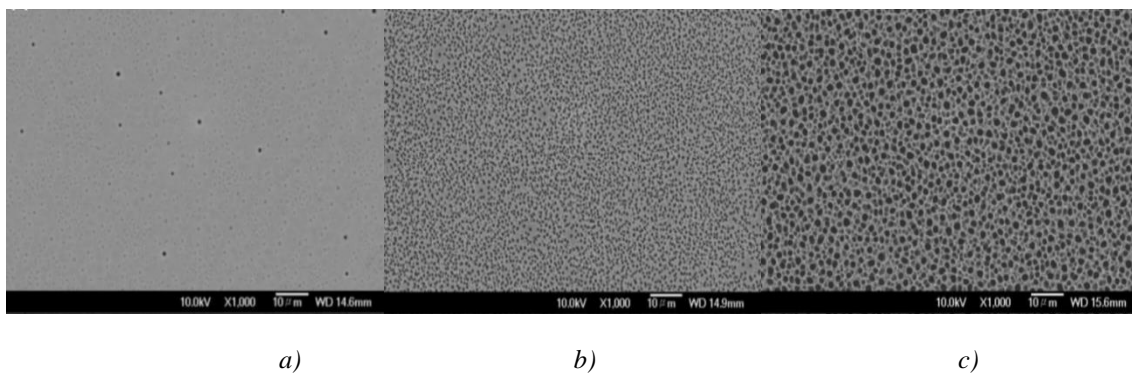


Fig.3. Etching time (a),(b) and (c) of FESEM for P-Si before irradiation .

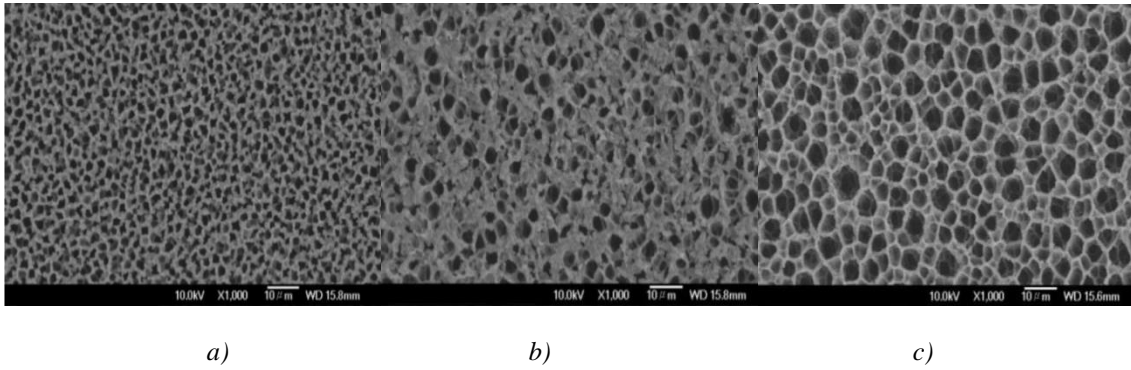


Fig.4. Etching time (a) 10min.), (b) 20min.) and (c) 30 min.) after irradiation of FESEM for P-Si .

b) Cross-section images of P-Si

Cross section of P-Si was investigated by Field emission scanning electron microscope with neutron flux density. Fig (5) illustrates cross section images of P-Si before irradiation, pore size increases with increasing etching. This because the further dissolution in P-Si layer with etching time and formation of connected pores. After irradiation , electrons confined within the thin walls increase which leads to increase in the number of pores also, we note appearance of columns like nanorods with irregular shapes up to depth(157.6 nm) compared with before irradiation (73.8nm).Penetration depth rate of pores increases with increasing etching [18] as Fig (6).

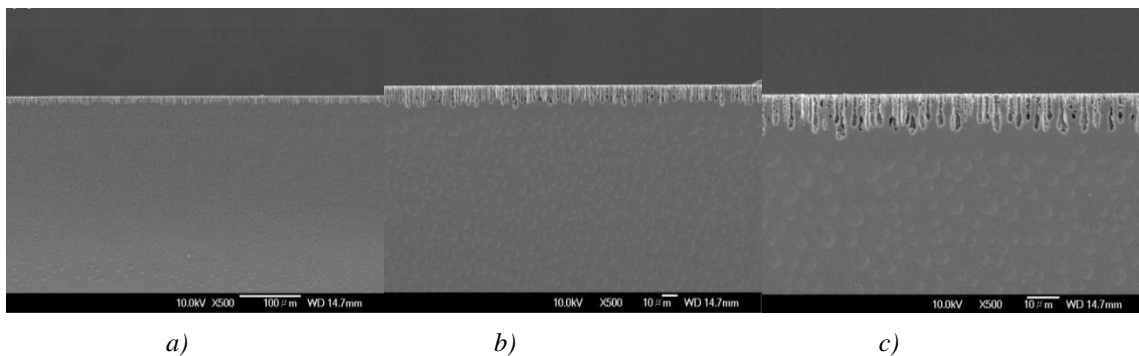


Fig. 5. Etching time(a₁), (b₁) and (c₁) of FESEM (cross section) for P-Si before irradiation.

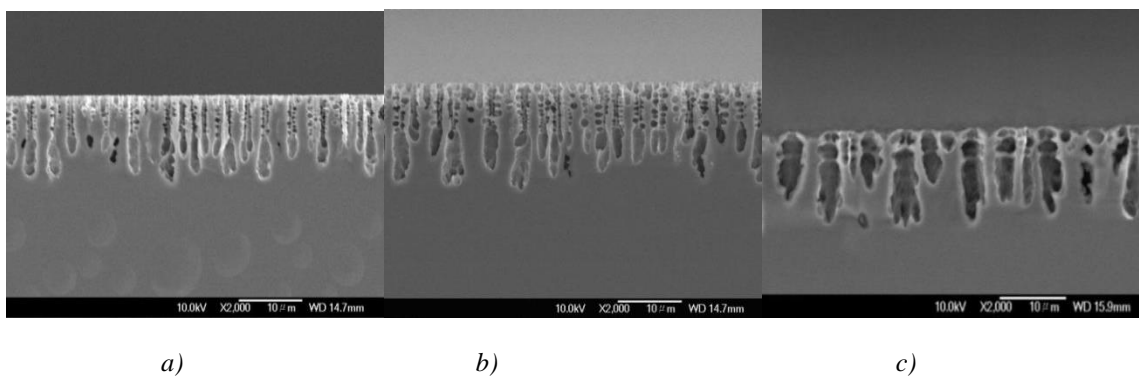


Fig.6. Etching time (a₁), (b₁) and (c₁) after irradiation of FESEM (cross section) for P-Si .

4. Conclusions

The XRD characteristics illustrate that the P-Si layers still in crystalline phase with small changing in the diffraction peak. These results indicate small shifting of diffraction peak with increasing etching time. The maximum diffraction peak (111) observed at $2\theta = 28.35^\circ$ before irradiation. While after irradiation, the maximum diffraction peak (200) investigated at $2\theta = 34.22^\circ$. This happens due to the change of phase. FESEM images (top surface and cross section) show that better crystalline behavior for the P-Si layer after irradiation. Furthermore, this irradiation results in increase pores width on P-Si surface.

References

- [1] S. Basu, J. Kaungo, Nanocrystalline Porous Silicon. Dept. of Electronic and Telecommunication Engineering, Jabalpur University, India, 2011.
- [2] B. Gelloz, R. Mentek, N. Koshlda, J. of Sol. Sci. and Tech. **3**(5), 83 (2014).
- [3] O. Bisia, S. Ossicinib, L. Pavesi, Science Reports **38**(3), 1 (2000).
- [4] A. Rothschild, Y. Komen, J. of App. Phys. **95**(2), 6374 (2004).
- [5] M. Prabhu, A. Sivanantham, P. Karthick, American Institute of Physics **531**(8), 1536 (2013).
- [6] L. Znaidi, T. Chauveau, A. Tallaire, Thin Solid films **617**(5), 156 (2016).
- [7] S. Jurablu, M. Farahmandjou, T. Firoozabadi, Journal of Science, Islamic Republic of Iran **26**(3), 281 (2015).
- [8] G. Choppin, J. Liljenzin, J. Rydberg, Butterworth-Heinemann, Woburn third edition, 2002.
- [9] P. Rinard, Technical Report NUREG/CR-5550, Nuclear Regulatory. Commission, 1991.
- [10] Johnston A., IEEE Trans. Nuclear. Science **60**(3), 2073 (2013).
- [11] G. Summers, E. Burke, S. Shapiro, IEEE Trans. Nuclear Science **40**(6), 1372 (1993).
- [12] K. Behzad, W. M. Yunus, Z. A. Talib, A. Zakaria, A. Bahrami, E. Shahriari, Journal of Materials **5**(3), 157 (2012).
- [13] C. G. Vayenas, E. White, Springer **39**(3), 145 (2012).
- [14] M. Q. Zayer, M. Sc. Thesis, University of Technology, Baghdad, 2010.
- [15] J. D. Ryckman, R. A. Reed, S. M. Weiss. Journal of Apply Physics **108**(11), 113 (2010).
- [16] K. A. Salman, Z. Hassan, K. Omer, International of Journal Electrochemical Sciences **7**(9), 376 (2012).
- [17] J. Kuendig, M. Goetz, J. Meier, E. Fernandez, In 16th EC Photovoltaic Solar Energy Conference, 986 (2000).
- [18] V. Paillard, P. Puech, M. A. Laguna, R. Carkes, B. Kohn, F. Huisken, Journal of Applied Physics **86**(4), 1921 (1999).